Article

Journal of
Nanoscience and Nanotechnology
Vol. 17, 2061–2066, 2017
www.aspbs.com/jnn

Synthesis and Catalytic Performance of HMCM-49/MCM-41 Composite Molecular Sieve for Alkylation of Phenol with Isopropanol

Liguo Wei[1,*], Dong Wang[2], Yongli Dong[1,*], Weina Song[1], Xiaoxu Liu[1], and Kunyao Song[1]

[1] College of Environmental and Chemical Engineering, Heilongjiang University of Science and Technology, Harbin 150022, P. R. China
[2] School of Chemical and Environmental Engineering, Hanshan Normal University, Chaozhou 521041, P. R. China

HMCM-49/MCM-41 composite molecular sieve was synthesized with hydrothermal method. The physicochemical properties of the composite were characterized by using XRD, FT-IR, SEM, N_2 isothermal adsorption–desorption and NH_3-TPD. Results of different characterizations indicated that the synthesized composite molecular sieve possessed the characteristics of both HMCM-49 and MCM-41. XRD and N_2 isothermal adsorption–desorption revealed that it has both micropores and mesopores, a larger surface area than that of HMCM-49, NH_3-TPD and pyridine adsorbed FT-IR revealed that the strong acidic sites that caused side reaction in HMCM-49 are deactivated in the composite molecular sieve of HMCM-49/MCM-41. When applied to the alkylation of phenol with isopropanol, the HMCM-49/MCM-41 composite molecular sieve exhibit an enhanced catalytic performance with significant enhancement in *p*-isopropylphenol and *o*-isopropylphenol selectivity, which can be ascribed to the composite characteristics of HMCM-49 and MCM-41. This kind of material will has widely industrial application in preparation of alkyl-phenol.

Keywords: Composite Molecular Sieve, MCM-41 Zeolites, HMCM-49 Zeolites, Alkylation of Phenol, Isopropylphenol.

1. INTRODUCTION

Alkyl-phenol such as *p*-isopropylphenol (*p*-IPP) and *o*-isopropylphenol (*o*-IPP) is an important intermediate of fine chemical. *p*-IPP has been widely used in the fields of wire-coatings, machinery cleanser, surfactants, synthetic resins, adhesives and pharmaceutical intermediates. Besides, *o*-IPP can also be employed as intermediates to synthesize leafhopper pesticides. Currently, alkyl-phenol were primarily synthesized from phenol with olefins, alcohols or chlorinated hydrocarbons through alkylation reactions using aluminum phenol $[Al(OC_6H_5)_3]$ as catalyst. However, significant shortcomings, such as complex operational process, low yield, erosion, pollution, separation difficulties, high cost and low mass production greatly hinder its industrial application. Therefore, developing a new green technology and catalyst to synthesize alkyl-phenol is of special attention in recent years.[1–3]

MCM-49 zeolites possess the same framework to that of MCM-22, which consists of three independent pore systems.[4,5] One pore system is composed of two-dimensional (2D) sinusoidal accessible channels through 10-membered ring (MR) (4.1×5.1 Å). And the second pore system contains 12-MR large supercages with an inner diameter of 7.1 Å and a height of 18.2 Å, which are connected by 10-MR apertures. The third one comprises a large hemisupercages ($7.0 \times 7.1 \times 7.1$ Å) on the external surface. Due to their unique structure and acid properties, MCM-49 zeolites have been extensively investigated in various catalysis fields.[6–9] Our previous works reveal that the HMCM-49 zeolites exhibit good catalytic performance in alkylation of phenol with isopropanol,[10,11] and the catalytic performance of HMCM-49 zeolites could be further improved by deactivating the strong acid sites where byproducts were produced, and to realize this, silane reagent $[(C_2H_5O)_4Si]$ was used to treat HMCM-49 zeolites via a CVD process.[12] However, the process of CVD is a long and complicated modification.

Composite molecular sieves, especially micro/mesoporous composite, have been paid much attention due to their synergistic performance in catalytic reactions.[13–16]

*Authors to whom correspondence should be addressed.

Most MCM-41 based composite molecular sieves were synthesized and applied in different catalytic reactions.[17–21] To the best of our knowledge, there have been no reports on synthesis and application of HMCM-49/MCM-41 composite molecular sieves to alkylation of phenol with isopropanol. Since MCM-41 is a mesopores zeolite with large surface area and moderate strength acid sites, after combined with HMCM-49, it is predicated to deactivate the strong acid sites of HMCM-49 and enlarge the surface areas of it. These were all benefit for improving the catalytic performance of HMCM-49 on the alkylation of phenol with isopropanol.

Therefore, in this paper we synthesized the HMCM-49/MCM-41 composite molecular sieves by hydrothermal method. The phase, morphology, structure, and acid properties of samples were well investigated by means of XRD, SEM, FT-IR, N_2 adsorption–desorption and NH_3-TPD. Meanwhile the catalytic performance on alkylation of phenol with isopropanol on HMCM-49/MCM-41 was also studied.

2. EXPERIMENTAL DETAILS

The materials and equipment used included the following: hexamethyleneimine (HMI, Kermel chemreagent Co., Ltd., Tianjin, China); sodium aluminate (Kermel chemreagent Co., Ltd., Tianjin, China); silica sol (Guolian Technology Co., Ltd., Jiangyin, China); Cetyltrimethylammonium bromide (Kermel chemreagent Co., Ltd., Tianjin, China); Tetraethyl orthosilicate (Kermel chemreagent Co., Ltd., Tianjin, China); and Ammonia solution (Kermel chemreagent Co., Ltd., Tianjin, China). All of the other chemicals and solvents in this work were commercially available and were used as received without further purification.

MCM-49 zeolites were obtained by the reported procedure.[22] The protonic form of MCM-49, denoted as HMCM-49, was obtained by ion-exchange of the as synthesized MCM-49 with aqueous NH_4NO_3 solution, and then calcined at 540 °C in air for 3 h.

To synthesize the HMCM-49/MCM-41 composite, a sol–gel of MCM-41 was firstly prepared according to a published procedure.[23] While stirring, a certain amount of HMCM-49 zeolite was added to the colloidal precursor of MCM-41. The mixture was then stirred for a few minutes, followed by hydrothermal crystallization at 100 °C for 48 h. After cooling to the room temperature, the resulting solid product was filtered, washed thoroughly with deionized water and dried at 120 °C. The composite samples were then obtained by calcining the product at 540 °C for 5 h in air. By varying the weight of HMCM-49 added to the MCM-41 gel, several HMCM-49/MCM-41 composite with different weight percents of HMCM-49 to MCM-41 gel were prepared, denoted as HM-49/M-41(x%), where x represents the theoretical weight percent of HMCM-49 to MCM-41 gel.

X-ray diffraction (XRD) experiments were carried out with Bruker D8 Advance diffractometer using Cu Kα radiation ($\lambda = 0.15405$ nm). The morphologies of samples were inspected on MX2600FE scanning electron microscope (SEM). The N_2 adsorption–desorption of samples was conducted on a micromeritics ASAP2020 surface area and pore size analyzer at −196 °C (liquid nitrogen temperature) using accompanying software from Micromertitics. The surface areas were calculated by using the conventional BET method, and the pore size diameters were calculated by using BJH method. The property of the acid sites was characterized by a Pyridine adsorbed FT-IR spectrometer. All spectra were measured at 180 °C. NH_3-TPD was performed on a self-designed apparatus. Prior to the measurement, 50 mg sample was first pretreated in Ar at 600 °C for 60 min, then cooled down to 100 °C and saturated at this temperature with ammonia until equilibrium. The NH_3-TPD profile was recorded with a thermal conductivity detector (TCD) with a heating rate of 10 °C/min from 100 to 600 °C under argon flow.

Alkylation of phenol with isopropanol was carried out on a fixed-bed, vertical-flow reactor with 40 cm in length and 0.5 cm in internal diameter. 0.5 g catalyst (20–30 mesh) was placed in the middle of the reactor and supported on either side with a thin layer of quartz wool and ceramic beads. The reactor was heated to the requisite temperature with the help of a tubular furnace controlled by a digital temperature controller-cum indicator. The reactants were fed into the reactor using a syringe injection pump (sage instruments) that could be operated at different flow rates. The reaction was carried out at atmospheric pressure. The bottom of the reactor was connected to a condenser and a receiver to collect the products. The products were collected at a time interval of 1 h after stability period. The products were analyzed on a gas chromatograph (GC-9890A) with a FID detector equipped with a 30 m length DB-1 capillary column using nitrogen as carrier gas.

3. RESULTS AND DISCUSSION

The crystal phase, pore size distribution, surface topography and chemical component of the composite molecular sieves HMCM-49/MCM-41 were characterization by XRD, N_2 adsorption–desorption and SEM measurement, in comparison with the corresponding HMCM-49 and MCM-41.

Figure 1 shows XRD patterns of the HMCM-49/MCM-41 composite with weight percents of HMCM-49 to MCM-41 gel from 1.0 to 5.0%. It can be observed from Figure 1(a) that the meso-structure is well formed when the weight percent of HMCM-49 to MCM-41 gel is lower than 3.0%. With an increase in the amount of HMCM-49 in the MCM-41 gel, the peak intensity of the MCM-41 decrease significantly. When the weight percent of HMCM-49 is increased to 5.0%, the characteristic peaks

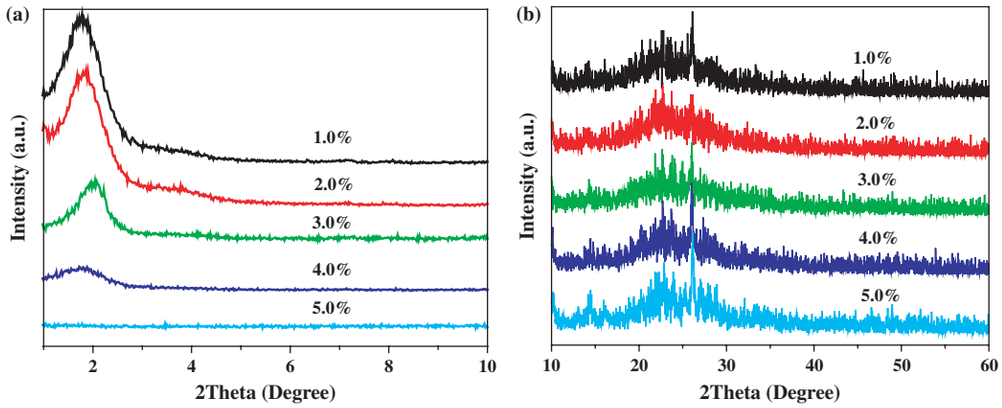

Figure 1. X-ray diffraction of HMCM-49/MCM-41 (x%) composite molecular sieves (a) low angle (b) high angle.

corresponding to MCM-41 can no longer be detected by XRD. This is ascribed to that adding too much HMCM-49 to MCM-41 gel may suppress the crystallization of MCM-41. As shown in Figure 1(b), the characteristic peak position of HMCM-49 shows no obvious change with increasing weight percent of HMCM-49 to MCM-41 gel and the HMCM-49 peak intensity increases slightly with an increasing amount of MCM-49 in the composite. The diffraction peaks of samples are well consistent with that of HMCM-49 reported in the literatures.[22, 24] It could be concluded from XRD analysis that when the weight percent of HMCM-49 to MCM-41 gel is 2.0%, both the meso-structure component of MCM-41 and the micro-structure component of HMCM-49 are well formed. Therefore, the HMCM-49/MCM-41 composite molecular sieve with HMCM-49 to MCM-41 gel percent ratio of 2.0% is selected for further investigation.

Figure 2 shows the SEM images of the composite molecular sieve HMCM-49/MCM-41 and the corresponding molecular sieve of HMCM-49 and MCM-41. MCM-41 shows irregular crystal morphology, whereas HMCM-49 shows numerous lamellar crystals made of thinner crystal layers. The HMCM-49/MCM-41 composite molecular sieve shows a unique aggregated crystal like morphology, which is clearly different from those of parent MCM-41 and HMCM-49. Furthermore, it could be found that meso-structure of MCM-41 was formed over HMCM-49 structure.

The N_2 adsorption–desorption isotherms of MCM-49/MCM-41 is exhibited in Figure 3, and the corresponding surface area and pore size parameters of HMCM-49/MCM-41 composite molecular sieves are summarized in Table I. As shown in Figure 3, the N_2 adsorption–desorption isotherms of HMCM-49/MCM-41 was similar to type I in the low pressure range ($p/p_0 < 0.05$), which is typical for microporous zeolites, and the adsorbed amount of N_2 was below 100 cm^3/g, which was the value of the filling volume of micropores. However, the N_2 adsorption–desorption isotherms of HMCM-49/MCM-41 were silimar to those of type IV in the pressure range ($p/p_0 > 0.05$), a typical of mesoporous molecular sieves and it indicated the existence of mesopores. In the pressure range ($p/p_0 < 0.40$), the adsorbed amount of N_2 increased linearly with pressure due to monolayer adsorption of N_2 on the walls of the pores, while in range of $0.40 < p/p_0 < 0.95$, there was a jump in the adsorbed amount appeared because N_2 began filling the mesopores. Multilayer adsorption of N_2 in the mesopores occurred when p/p_0 became higher.

It can be found from Table I that HMCM-49/MCM-41 composite molecular sieves have high specific surface areas (373.13 m^2/g) and large pore volumes (0.67 cm^3/g), which is smaller than pure MCM-41 and

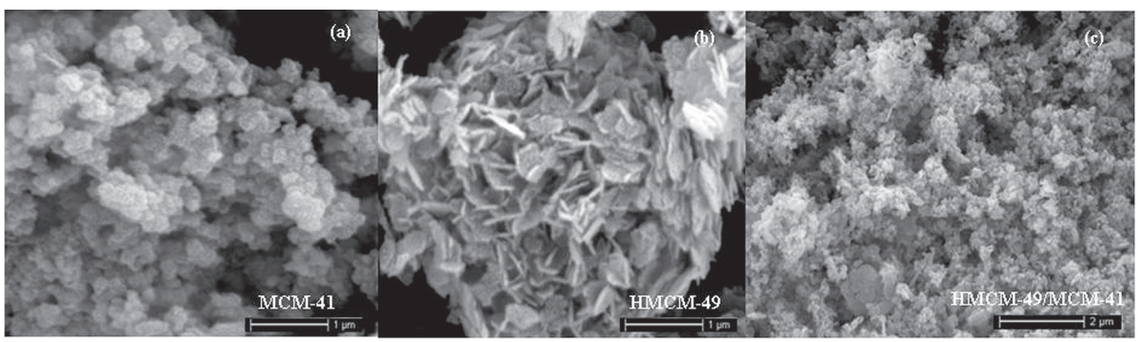

Figure 2. SEM images of samples (a) MCM-41 (b) HMCM-49 (c) HMCM-49/MCM-41.

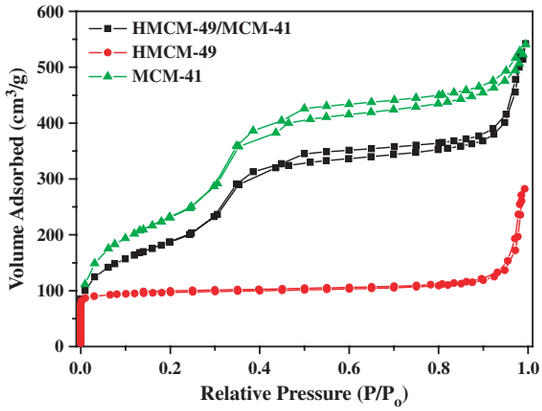

Figure 3. N_2 adsorption–desorption isotherms of HMCM-49/MCM-41, MCM-41 and HMCM-49.

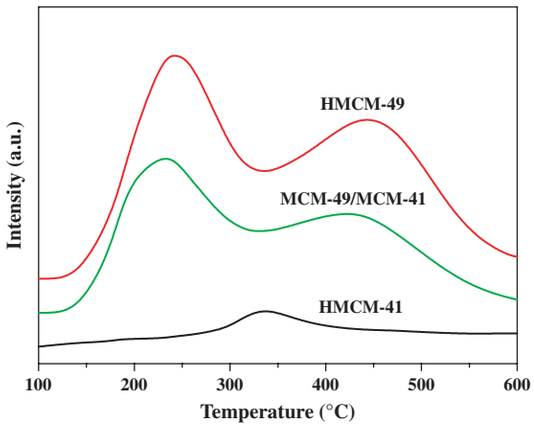

Figure 4. NH_3-TPD patterns of HMCM-49/MCM-41, MCM-41 and HMCM-49.

lager than pure HMCM-49, respectively. These results may attribute to the simultaneous existence of HMCM-49 and MCM-41 nanoparticles in HMCM-49/MCM-41 composite molecular sieves.

Figure 4 shows the NH_3-TPD patterns of HMCM-49/MCM-41, MCM-41 and HMCM-49. For MCM-41, only one weak desorption peak is detected at about 350 °C, which can be attributed to desorption of ammonia from the moderate acidic sites. For HMCM-49 and the composite molecular sieve HMCM-49/MCM-41, it can be seen that each sample consists of two broad desorption peaks in 200–300 °C and 400–500 °C, corresponding to the low-temperature desorption peak at the weak acid sites and the high-temperature desorption peak at the strong acid sites, respectively.[25] It should be noted that the strong acid peak of HMCM-49 shifts to lower temperature and weak acid peak doesn't change greatly after composited with MCM-41. Additionally, both desorption peaks area, especially strong acid peak reduces markedly after composition. The result indicates that the composite molecular sieve can greatly decrease the acid sites, especially the strong acid sites of HMCM-49 zeolites.

In order to further study the changed acid properties of the composite molecular sieve HMCM-49/MCM-41 compared with HMCM-49, the acidity of HMCM-49 and HMCM-49/MCM-41 were examined by FT-IR spectroscopy using the pyridine adsorption technique, as show in Figure 5. The band of 1450 cm^{-1} is assigned to the protonated pyridine (PyH^+) molecules adsorbed on Lewis acid sites, the band of 1540 cm^{-1} is ascribed to the protonated pyridine (PyH^+) molecules adsorbed on Brønsted acid sites; and the band of 1490 cm^{-1} is related with the protonated pyridine (PyH^+) molecules adsorbed on both Brønsted and Lewis acid sites.[26] From Figure 5, it can be seen that both Brønsted and Lewis acid sites of the composite molecular sieve HMCM-49/MCM-41 decrease compared with HMCM-49, and the Brønsted acid sites decreased more rapidly. This is in agreement with the results of NH_3-TPD characterization. There are almost no acidic sites over the surface of the pure silica molecular sieve of MCM-41, therefore the acidic sites detected by FT-IR are mainly provided by HMCM-49 and the Brønsted acid sites of HMCM-49 can be modified after composited with MCM-41.

Alkylation of phenol with isopropanol over molecular sieve is a green route to prepare *p*-isopropylphenol (*p*-IPP) and *o*-isopropylphenol (*o*-IPP), the synthesis routes are shown in Scheme 1. In the previous works we found that alkylation of phenol with isopropanol is an acid catalytic reaction, the HMCM-49 molecular sieve exhibits good catalytic performance on this reactions

Table I. Physical property of pure molecular sieves and HMCM-49/MCM-41 composite.

Samples	BET surface area (m^2/g)	Pore size (nm)	Pore volume (cm^3/g)
MCM-41	722.14	3.54	0.74
HMCM-49	291.27	0.41	0.58
HMCM-41/MCM-49	373.17	2.85	0.67

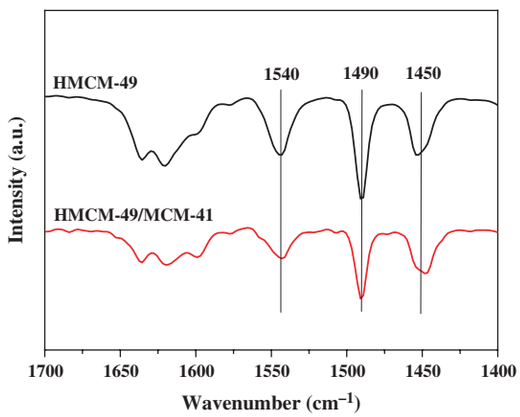

Figure 5. FT-IR with pyridine adsorption of HMCM-49/MCM-41 and HMCM-49.

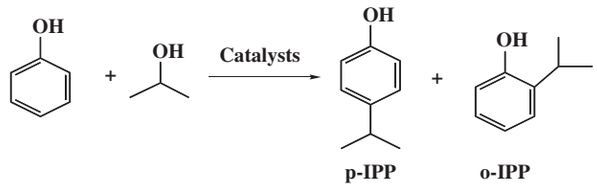

Scheme 1. Main reactions of phenol with isopropanol over zeolite catalysts.

and its catalytic performance could be further improved by deactivating the strong acid sites where byproducts were produced.[10–12] As discussed above, the composite molecular sieve HMCM-49/MCM-41 shows a modified pore structure and deactivates the strong acid sites of HMCM-49, which is expected to enhance the catalytic performance on alkylation of phenol with isopropanol. Therefore, catalytic performance of HMCM-49/MCM-41 were tested under the reaction conditions of $T = 180$ °C, $WHSV = 3.0\ h^{-1}$, and $n_{IPA}/n_{Phenol} = 0.8$, for comparing, the catalytic performance of HMCM-49 was also tested under the same conditions.

As shown in Figure 6, the conversion of phenol and the selectivity of *o*-isopropylphenol and *p*-isopropylphenol are all increased when the composite molecular sieve HMCM-49/MCM-41 was used. The results reveal that acid sites especially strong Brønsted acid sites on the surface of HMCM-49 lead to side reactions and could be eliminated efficiently after composition with MCM-41, and thereby the selectivity of *o*-isopropylphenol and *p*-isopropylphenol increases. Meanwhile, the increase of the conversion of phenol is ascribed to that the BET surface area of the composited molecular sieve HMCM-49/MCM-41 is larger than that of HMCM-49. Meanwhile, a higher yield of *o*-isopropylphenol and *p*-isopropylphenol were obtained. As shown in Figure 7, the yield of *o*-isopropylphenol and *p*-isopropylphenol over the HMCM-49/MCM-41 composite molecular sieve are 41.6% and 13.3%, respectively, which are all higher than that over the pure HMCM-49

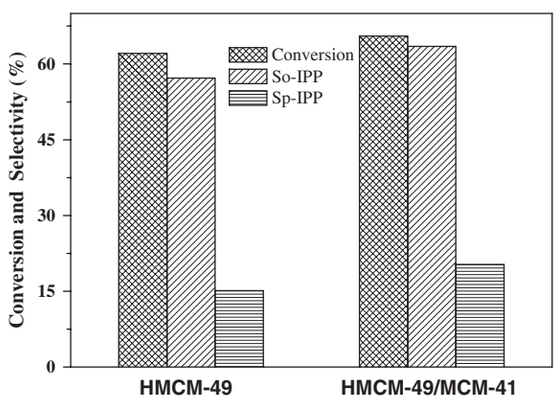

Figure 6. Catalytic performance of HMCM-49/MCM-41 and HMCM-49 on alkylation of phenol with isopropanol. So-IPP: selectivity of *o*-isopropylphenol, Sp-IPP: selectivity of *p*-isopropylphenol.

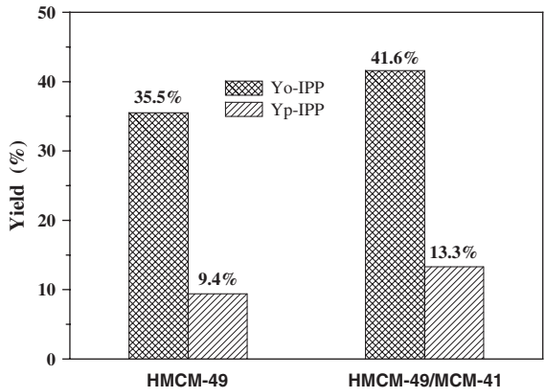

Figure 7. Yields of *o*-isopropylphenol and *p*-isopropylphenol over HMCM-49/MCM-41 and HMCM-49 catalysts. Yo-IPP: yield of *o*-isopropylphenol, Yp-IPP: yield of *p*-isopropylphenol.

Table II. Distribution of alkylation products over HMCM-49/MCM-41 and HMCM-49.

		Selectivity (%)				
Catalysts	Conversion(%)	$S_{o\text{-IPP}}$	$S_{p\text{-IPP}}$	S_{DIPP}	S_{TIPP}	S_{IPPE}
HMCM-49	62.1	57.2	15.1	19.0	5.4	3.3
HMCM-49/MCM-41	65.5	63.5	20.3	9.8	1.3	5.1

molecular sieve. This further confirms that the catalytic performance of HMCM-49 is enhanced after composition with MCM-41.

Products of phenol alkylation with isopropanol on HMCM-49/MCM-41 and HMCM-49 are summarized in Table II. Besides the main product *o*-isopropylphenol and *p*-isopropylphenol, several undesired products such as diisopropylphenols (2,6-DIPP, 2,4-DIPP, 2,5-DIPP, 3,5-DIPP) and triisopropylphenols (2,4,6-TIPP) was formed during alkylation of phenol with isopropanol over catalysts used here. The by-product of further alkylation products such as diisopropylphenols and triisopropylphenols decreased after composited with MCM-41, which further indicates that acid sites especially strong Brønsted acid sites on the surface of HMCM-49 that lead to side reactions could be eliminated efficiently when it was combined with MCM-41. While the by-product of phenylisopropyl ether (IPPE) increased after composited with MCM-41 is also due to strong Brønsted acid sites are eliminated and weak acid sites which lead to produce IPPE becomes dominant,[27] and meanwhile aperture of composite micro-meso-pore and the dimensional size around the pore mouths may be suitable to form IPPE.

4. CONCLUSION

In summary, the HMCM-49/MCM-41 composite molecular sieve was successfully synthesized by hydrothermal method. This composite molecular sieve has both micropore and mesopore structure, and a larger surface

area than that of HMCM-49. Especially, this composite molecular sieve can effectively eliminate or deactivate most of the strong Brønsted acid sites of HMCM-49 which lead to side reaction. Hence the catalytic performance of HMCM-49 on alkylation of phenol with isopropanol was improved and the selectivity of *p*-isopropylphenol and *o*-isopropylphenol are significantly enhanced. The enhanced catalytic performance can be ascribed to the composite characteristics of HMCM-49 and MCM-41. This type of catalyst is anticipated to arouse broad interest in further boosting the catalytic performance of phenol alkylation with isopropanol by compositing different classes of molecular sieves. And it will have widely industrial application in preparation of alkyl-phenol.

Acknowledgments: The authors acknowledge the financial support from National Natural Science Foundation of China (Grant No. 21203058 and 51307046), the National key Technology Support Program of China (No. 2013BAE04B03), the Science Foundation for Youths of Heilongjiang Province of China (Grant Nos. QC2016013, OC2011C106), the Foundation of Educational Commission of Heilongjiang Province of China (No. 12531579), the Innovative Talents Program of Heilongjiang University of Science and Technology (Q20130202) and the Project of Institute of Higher Education of Heilongjiang Province (HGJXH C110919).

References and Notes

1. R. Z. Zhu, C. W. Guo, X. H. Tang, and L. R. Pan, *Chem. J. Chinese U* 120, 1615 (**1999**).
2. D. Wang, X. Li, Z. Liu, Y. Zhang, Z. Xie, and Y. Tang, *J. Colloid Interf. Sci.* 350, 290 (**2010**).
3. W. Xu, S. J. Miller, P. K. Agrawal, and C. W. Jones, *Appl. Catal. A: Gen.* 459, 114 (**2013**).
4. M. E. Leonowicz, J. A. Lawton, S. L. Lawton, and M. K. Rubin, *Science* 264, 1910 (**1994**).
5. S. L. Lawton, M. E. Lenowicz, R. D. Partrideg, P. Chu, and M. K. Rubin, *Micropor. Mesopor. Mat.* 23, 109 (**1998**).
6. K. Liu, S. Xie, S. Liu, G. Xu, N. Gao, and L. Xu, *J. Catal.* 283, 68 (**2011**).
7. C. Sun, S. Yao, W. Shen, and L. Lin, *Micropor. Mesopor. Mat.* 122, 48 (**2009**).
8. S. Yao, C. Sun, J. Li, X. Huang, and W. Shen, *J. Nat. Gas Chem.* 19, 1 (**2010**).
9. K. Liu, S. Xie, G. Xu, Y. Li, S. Liu, and L. Xu, *Appl. Catal. A: Gen.* 383, 102 (**2010**).
10. L. G. Wei, Y. C. Shang, and P. P. Yang, *React. Kinet. Catal. L* 93, 265 (**2008**).
11. L. G. Wei and Y. C. Shang, *Petro. Tech.* 38, 656 (**2009**).
12. L. Zhang, L. G. Wei, L. Wang, and Y. C. Shang, *Reac. Kinet. Mech. Cat.* 110, 215 (**2013**).
13. W. Yu, P. Yuan, D. Liu, L. Deng, W. Yuan, B. Tao, H. Cheng, and F. Chen, *J. Hazard. Mater.* 285, 173 (**2015**).
14. Y. Wang, W. Wang, Y. Chen, J. Zheng, and R. Li, *J. Fuel Chem. Tech.* 41, 873 (**2013**).
15. S. Zhu, S. Liu, H. Zhang, E. Lu, and J. Ren, *Chinese J. Catal.* 35, 1676 (**2014**).
16. Q. Zhang, C. Li, S. Xu, and H. Shan, *J. Porous Mater.* 20, 171 (**2013**).
17. H. Li, S. He, K. Ma, Q. Wu, Q. Jiao, and K. Sun, *Appl. Catal. A: Gen.* 450, 152 (**2013**).
18. T. Jiang, L. Qi, M. Ji, H. Ding, Y. Li, Z. Tao, and Q. Zhao, *Appl. Clay Sci.* 62, 32 (**2012**).
19. Q. Tang, H. Xu, Y. Zheng, J. Wang, H. Li, and J. Zhang, *Appl. Catal. A: Gen.* 413, 36 (**2012**).
20. Y. Li, W. Zhang, X. Wang, Y. Zhang, and T. Dou, *J. Porous Mater.* 15, 133 (**2015**).
21. B. R. Jermy, M. A. B. Siddiqui, A. M. Aitani, and M. R. Saeed, *J. Porous Mater.* 19, 499 (**2012**).
22. J. M. Bennett, C. D. Chang, and S. L. Lawton, US Patent, 5236757 (**1993**).
23. W. L. Huang, B. J. Liu, F. M. Sun, Z. H. Zhang, and X. J. Bao, *Micropor. Mesopor. Mater.* 94, 254 (**2006**).
24. M. K. Rubin and P. Chu, US Patent, 4954325 (**1990**).
25. D. Nuntasri, P. Wu, and T. Tatsumi, *J. Catal.* 213, 272 (**2003**).
26. H. Knöuzinger, *Adv. Catal.* 25, 184 (**1976**).
27. R. F. Parton, J. M. Jacobs, H. Van Ooteghem, and P. A. Jacobs, *Stud. Surf. Sci. Catal.* 46, 211 (**1989**).

Received: 15 October 2015. Accepted: 29 March 2016.